CHEMISTRY OF MATERIALS

ARTICLE

pubs.acs.org/cm

Tuning the Light Absorption of $Cu_{1.97}S$ Nanocrystals in Supercrystal Structures

Ilka Kriegel,[†] Jessica Rodríguez-Fernández,[†] Enrico Da Como,[†,*] Andrey A. Lutich,[†] Johann M. Szeifert,[‡] and Jochen Feldmann[†]

[†]Photonics and Optoelectronics Group, Department of Physics and CeNS, Ludwig-Maximilians-University, 80799 Munich, Germany

[‡]Department of Chemistry, Ludwig-Maximilians-University, 81377 Munich, Germany

Supporting Information

ABSTRACT:

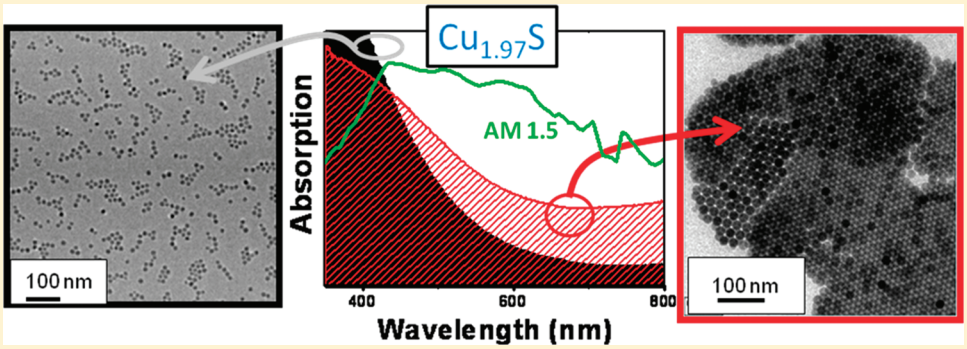

We report on tuning the light absorption properties of $Cu_{1.97}S$ nanocrystals upon organization in ordered supercrystal structures. In particular, we show that the weak absorption profile of $Cu_{1.97}S$ nanocrystals can be tuned toward the red part of the visible spectrum. We demonstrate that the controlled addition of ligands to the supercrystals can be used to trigger nanocrystal deassembly, leading to the recovery of the optical properties of the isolated nanocrystals and thus, to a lower absorption in the red part of the spectrum. Supported by structural characterization via electron microscopy and X-ray diffraction our results suggest that the tuning is primarily a consequence of nanocrystal close-packing. Our results highlight an effective approach for extending the light absorption characteristics of $Cu_{1.97}S$ nanocrystals toward the visible that may be relevant for their application in nanocrystal-based photovoltaics.

KEYWORDS: nanocrystals, copper sulfide, supercrystals, assembly, absorption, light-harvesting

INTRODUCTION

The need for new materials relevant for energy conversion and extracted from earth-abundant elements has recently changed the focus of attention in photovoltaic research, toward unexplored systems and new preparation strategies.[1] Many combinations of abundant elements can in principle create semiconductor materials,[1−3] which are the building blocks for solar and fuel cells or photocatalytic devices. Earth abundant materials with appealing processing characteristics may, however, exhibit poor stability or an undesirable electronic structure for achieving good carrier transport or optical absorption. The combination of copper and sulfur has been highlighted as a material for sustainable photovoltaics.[1,4] Recently, it has been further shown that nanocrystals (NCs) of Cu_2S can be used in solar energy applications[1,4] with the advantages of colloidal NC-based solar cells.[5−7] However, a drawback of Cu_2S, and some of its derived copper deficient structures $Cu_{2-x}S$, is the indirect bandgap, which unfortunately precludes the full exploitation of the low optical gap (~1.2 eV for Cu_2S) in applications demanding good light harvesting properties in the visible. Because of this, copper sulfide NCs often exhibit light absorption in the blue part of the spectrum,[8] but only little coverage of the visible and near-infrared, where the solar spectrum has the maximum photon fluence.

Here, we show that the spontaneous self-assembly of $Cu_{1.97}S$ NCs into close-packed supercrystal arrays can tune their light absorption toward the red part of the visible spectrum. Our results highlight the potential of supercrystal structures made out of copper sulfide NCs for photovoltaic and photocatalytic processes, where the optimization of light absorption in the visible range is central for obtaining high photoconversion efficiencies.

EXPERIMENTAL METHODS

Chemicals. Copper(II) chloride ($CuCl_2 \cdot 2H_2O$, 99%) was purchased from Aldrich and sodium oleate ($CH_3(CH_2)_7CH{=}CH(CH_2)_7COONa$,

Received: November 23, 2010
Revised: February 11, 2011
Published: March 08, 2011

dx.doi.org/10.1021/cm103355e | *Chem. Mater.* 2011, 23, 1830–1834

95%) was acquired from TCI Europe. Dodecanethiol (DDT, $CH_3(CH_2)_{11}SH$, 98%) and oleylamine (OA, $CH_3(CH_2)_7CH{=}CH(CH_2)_8NH_2$, 90%) were supplied by Acros Organics. Poly(methylmethacrylate) (PMMA, M_w 120 000 g/mol) was procured from Sigma Aldrich. Pure grade ethanol and toluene were used in all preparations. All chemicals were used as received.

Synthesis of $Cu_{1.97}S$ Nanocrystals. Copper sulfide nanocrystals were synthesized as described elsewhere from the thermolysis of a Cu-oleate complex in a mixture of oleylamine and dodecanethiol.[9] First a Cu-oleate complex was obtained by reacting copper chloride (5.45 g) and sodium oleate (24.35 g) in a solvent mixture composed of 80 mL of ethanol, 60 mL of water and 140 mL of hexane. The reaction was carried out at ~60 °C for four hours. The organic layer containing the green Cu-oleate complex was washed three times with 100 mL of distilled water in a separatory funnel. Hexane evaporation yielded a green solid Cu-oleate complex. For the synthesis of 12.5 nm nanocrystals, 0.318 g of the Cu-oleate complex were dissolved in a solvent mixture containing 5 mL of oleylamine and 5 mL of dodecanethiol at room temperature. The addition of dodecanethiol led to a color change from dark green to turbid white, indicating the reduction of Cu^{II} to Cu^{I} by the sulfur compound. Subsequently the reaction mixture was heated to 230 °C under a nitrogen flow and reacted at this temperature for 6 min. During reaction the solution gradually changed from yellow to dark red, finally yielding a deep-brown turbid solution of copper sulfide nanocrystals. To wash the sample, we added 10 mL of toluene and 10 mL of a nonsolvent (ethanol), followed by centrifugation for 10 min at ~2.5 rcf. The deep brown precipitate was finally redispersed in 10 mL of toluene and typically consisted of close-packed supercrystal arrays. Note that sample washing was not performed in a glovebox. Air exposure typically induces the creation of copper deficiencies in Cu_2S, which may explain the final $Cu_{1.97}S$ structure of the as-prepared nanocrystals.

Nanocrystal Deassembly. The deassembly of the as-prepared $Cu_{1.97}S$ nanocrystals into stable colloidal dispersions was triggered by the careful addition of oleylamine, which strongly binds to the nanocrystal surface. Typically, 40 μL of oleylamine were added to 2 mL of the supercrystals in toluene, followed by simultaneous bath sonication and mild heating (ca. 40 °C) for several minutes. This resulted in stable colloidal dispersions of the $Cu_{1.97}S$ nanocrystals. Prior to TEM, DLS, FTIR and XRD characterization of the well-dispersed $Cu_{1.97}S$ nanocrystals, the large OA excess was reduced by the addition of a nonsolvent (ethanol), precipitation via centrifugation (10 min at ~2.5 rcf) and redispersion in toluene. The process was repeated three times. Optical density measurements have shown no changes in the spectra during the washing process, confirming that colloidal stability was retained.

Film Preparation. Poly(methylmethacrylate) films containing either supercrystals or well-dispersed $Cu_{1.97}S$ nanocrystals were prepared as follows. First, nanocrystals/supercrystals were precipitated from a 1.5 mL dispersion as described above. The precipitate was then redispersed in 0.5 mL of a toluene solution containing PMMA (10 mg/mL) and finally drop-casted onto clean quartz substrates.

Characterization. Absorption spectra of well-dispersed copper sulfide nanocrystals and supercrystals in PMMA films were measured with an integrating sphere in a UV−vis spectrophotometer (Hitachi U-3501). This allowed us to directly access absorption with no contributions from light scattering. Extinction spectra of the nanocrystals/supercrystals in toluene were measured in 1 cm path length quartz cuvettes on a Cary 5000 UV−vis−NIR spectrophotometer. Transmission electron microscopy was performed on a JEOL JEM-1011 microscope operating at 100 kV. HRTEM and electron diffraction were carried out on a FEI Titan 80−300 microscope operating at 300 kV. Samples for TEM/HRTEM characterization were prepared by placing 5 μL of diluted nanocrystal/supercrystal dispersions in toluene onto a carbon-coated copper grid/holey carbon film, respectively. The solvent excess was carefully removed with a filter paper after ca. 30 s. Dynamic light scattering (DLS) measurements were performed on a Zetasizer Nano S (Malvern Instruments, Malvern UK) with a 4 mW He−Ne laser operating at 633 nm and a detection angle of 173°. All measurements were carried out at 25 °C. The samples were diluted in filtered toluene (PTFE filters, 0.45 μm pore size) toluene for DLS characterization. Fourier transform infrared spectroscopy (FTIR) was performed on a Hyperion 2000 FTIR microscope (Bruker Optics, Ettlingen, Germany) operating in transmission mode. Samples for FTIR characterization were prepared by drop-casting well-dispersed $Cu_{1.97}S$ nanocrystals/supercrystals in toluene on a calcium fluoride (CaF_2) slide and allowed to dry at room temperature. The laser beam was focused on areas of high nanocrystal/supercrystal concentration and the interferogram was detected with a HgCdTe detector. Spectra (240 scans) were taken with a resolution of 4 cm^{-1} from 7500 to 600 cm^{-1} and corrected for water vapor and carbon dioxide absorption. X-ray diffraction (XRD) analysis was carried out in reflection mode using a Bruker D8 Discover diffractometer with Ni-filtered CuKα-radiation. Samples for XRD were prepared by drop-casting a concentrated dispersion of $Cu_{1.97}S$ nanocrystals/supercrystals onto a silicon substrate.

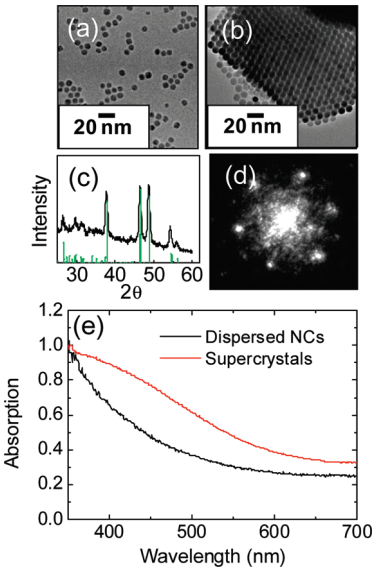

Figure 1. (a, b) TEM micrographs of 12.5 nm $Cu_{1.97}S$ NCs in the dispersed and supercrystal form. (c) Powder XRD pattern of the well-dispersed NCs. The green bars correspond to reference XRD pattern of $Cu_{1.97}S$ (JPCDS 20−0365). (d) Small-angle electron diffraction pattern of the supercrystals. (e) Normalized absorption spectra of $Cu_{1.97}S$ NCs and supercrystals in PMMA films.

RESULTS AND DISCUSSION

The solutions consisting of $Cu_{1.97}S$ NCs spontaneously self-assembled in micrometer-sized supercrystals have been studied from the structural and morphological point of view. Here, by supercrystals we define a close-packed ordered arrangement of NCs.[10] Stable dispersions of the as-prepared samples can be obtained upon addition of oleylamine in excess as we describe below. Those dispersions typically consist of well-dispersed (nonclose-packed) spherical NCs with a high degree of monodispersity, as shown in the TEM micrograph of Figure 1a. The powder XRD pattern of the NCs, black curve in Figure 1c, reveals that our NCs have a djurleite structure identical to that of bulk $Cu_{1.97}S$ (see reference diffraction pattern of $Cu_{1.97}S$, JPCDS 20−0365, green bars).

dx.doi.org/10.1021/cm103355e |Chem. Mater. 2011, 23, 1830–1834

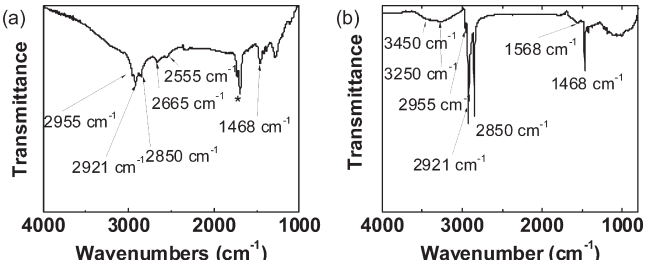

Figure 2. FTIR spectra of $Cu_{1.97}S$ supercrystals (a) before and (b) after oleylamine-induced deassembly. The NC size is 12.5 nm. In both cases the antisymmetric (2955 and 2921 cm^{-1}) and symmetric (2850 cm^{-1}) vibrations due to the aliphatic alkyl chains are observed. The peak at 1468 cm^{-1} is associated with the C−H bending mode. See text for the assignment of the most relevant peaks of the ligands.

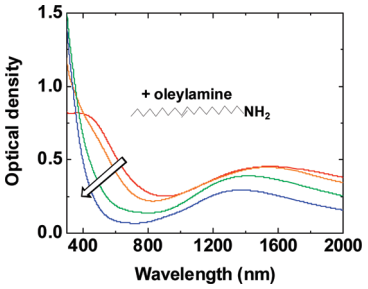

Figure 3. Evolution of the optical density spectrum of $Cu_{1.97}S$ supercrystals in toluene upon addition of oleylamine. The spectra were recorded at intervals of 1 min from the red to the blue curve.

A typical supercrystal arrangement is shown in the TEM micrograph of Figure 1b. The small-angle electron diffraction pattern of Figure 1d shows the reflections at small angles characteristic of ordered NC arrays.[11,12] A careful analysis of the TEM micrographs reveals that the $Cu_{1.97}S$ NCs tend to pack with a preferred orientation (see Figure S1 in the Supporting Information) into close-packed layers that further stack into multilayer supercrystals, as observed for CdSe and CdTe.[12,13] The origin of the self-assembly may be due to depletion-attraction forces,[14,15] or dipole moments present in the NCs.[16] We observed that the size (typically from 500 to 1000 nm) and shape of the supercrystals is rather arbitrary, although related to NC monodispersity. In general, the higher their monodispersity is, the higher their self-assembly efficiency and hence the supercrystals' size. From our data, we estimate that ca. 40×10^3 $Cu_{1.97}S$ nanocrystals (12.5 nm) constitute a 600 nm diameter supercrystal. The black curve in Figure 1e corresponds to the absorption spectrum of a diluted dispersion of 12.5 nm $Cu_{1.97}S$ NCs in a PMMA film. The absorption profile decreases steeply from the UV toward the blue, while the absorption in the rest of the visible is weak and overlapped by a broad background increasing toward the near-infrared. The latter has been recently ascribed to positive free carrier absorption (plasmon band),[17] in agreement with previous studies.[18] The typical weak absorption in the visible of the nonclose-packed NCs is significantly enhanced toward the visible in the supercrystals (red curve). The supercrystal spectrum shows a prominent band at 400 nm, which extends in the red up to 700 nm, whereas the residual absorption increasing toward the near-infrared is due to free carriers, as mentioned above. Here, we point out that all the experiments of Figure 1e were performed measuring the absorption of NCs/supercrystals in PMMA films mounted inside an integrating sphere. This allowed us to measure absorption excluding scattering contributions. Considering that the sample absorption (A) is expressed by the formula $A = 1 - (T + S)$, where T is the transmitted and S the scattered light from the sample, we can access directly the absorption, taking into account the scattered photons collected in the sphere. Our results prove that on an ensemble level the absorption profile of $Cu_{1.97}S$ NCs can be tuned toward the red part of the visible spectrum upon arrangement into close-packed structures, such as supercrystals. This absorption in the visible may be of importance for the improvement of the light harvesting properties of $Cu_{1.97}S$ NCs in solar energy conversion applications.

To investigate further the role of close-packing on the optical properties of $Cu_{1.97}S$ NCs, we have monitored the modifications in the optical density spectrum during NC deassembly. The deassembly process was typically triggered by the addition of an oleylamine excess, even though similar results were also obtained with an excess of dodecanethiol. In a typical experiment, 40 μL of oleylamine were added to 2 mL of the supercrystals dispersed in toluene, followed by simultaneous bath sonication and mild heating (ca. 40 °C) for several minutes. This resulted in stable colloidal dispersions of $Cu_{1.97}S$ NCs. The FTIR spectrum of the $Cu_{1.97}S$ NCs self-assembled into close-packed supercrystal arrays (Figure 2a) shows modes at 2555 and 2665 cm^{-1} characteristic of the S−H vibration. This suggests that dodecanethiol not only acts as a sulfur source during the synthesis, but also as a capping ligand. The S−H vibrational pattern is no further detected after oleylamine-triggered deassembly (Figure 2b). At the same time the $-NH_2$ scissoring mode at 1568 cm^{-1} and the antisymmetric and symmetric vibration modes of −N−H are observed between 3500 and 3300 cm^{-1}.[19] These results confirm that the ligand exchange from dodecanethiol to oleylamine occurs after the addition of an oleylamine excess. Figure 3 shows the evolution of the optical density spectrum of $Cu_{1.97}S$ supercrystals, during deassembly in intervals of 1 min. This experiment was performed with the NCs in solution and therefore it was not feasible to measure absorption in the integrating sphere. Hence, in Figure 3 we plot the optical density as the logarithm of T, where $T = 1 - (A + S)$. Even though a contribution from light scattering cannot be excluded, the general spectroscopic behavior of Figure 1(e) is reproduced. We note here that prior to each measurement, the sample was gently shook/sonicated to guarantee no supercrystal sedimentation during measurement. Upon deassembly, the visible part of the supercrystal spectrum (red curve) is gradually weakened (orange and green curves) and the resulting spectral profile after complete deassembly (blue curve) resembles the one of the isolated NCs. We point out here that the contribution of oleylamine to the optical density spectrum is negligible in the investigated spectral range.

The oleylamine-induced deassembly was further confirmed by dynamic light scattering (DLS) measurements (Figure 4). Initially (panel a), the supercrystals exhibit an average hydrodynamic size of about 1000 nm. After complete deassembly (panel b) the size distribution clearly narrows and shifts down to ∼17 nm, the hydrodynamic diameter of the constituent NCs. Since the concentration of material ($Cu_{1.97}S$ NCs) is kept constant throughout the deassembly process, the changes in optical density shown in Figure 3 do not originate from variations in material concentration but rather from the close-packing. Furthermore, the addition of oleylamine seems to have no influence on the crystalline structure of the NCs (see Figure S2 in the Supporting Information). These results further suggest that the tunability of the optical properties toward the visible is due to NC close-packing.

dx.doi.org/10.1021/cm103355e |*Chem. Mater.* 2011, 23, 1830–1834

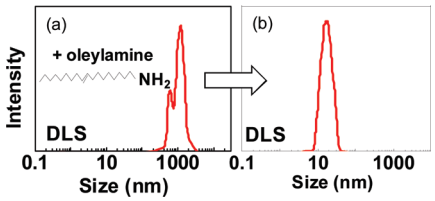

Figure 4. DLS size distributions of $Cu_{1.97}S$ supercrystals before (a) and after (b) complete deassembly triggered by addition of oleylamine.

In bulk $Cu_{1.97}S$ single crystals show a direct gap at ~496 nm (2.5 eV), whereas the indirect optical gap is located at 954 nm (1.3 eV).[18] Therefore, it is conceivable that the steep absorption starting at about 500 nm in the spectrum of the dispersed NCs is due to a direct transition of $Cu_{1.97}S$. Zhao et al. have recently reported on the optical properties of CuS, $Cu_{1.8}S$ and $Cu_{1.97}S$ NCs prepared by different chemical methods.[17] Changes in the light absorption features were interpreted considering quantum size effects, probed by varying NC size. In our samples, we did not observe pronounced size quantization effects, because of the large dimensions (>10 nm in diameter) compared to the estimated Bohr radius (3−5 nm).[20] Although similar effects have been reported for CdS nanoparticles,[21] a detailed description of the electronic structure for $Cu_{2-x}S$ NCs assemblies has not been reported yet. We propose here that the conduction and valence band wave functions of nearest-neighbor NCs may interact forming mini-bands upon close-packing in supercrystals. This could lead to a new electronic structure in which indirect transitions can become optically allowed by Brillouin zone folding,[22] a phenomenon extensively studied in superlattices of indirect semiconductors such as Si/Ge.[23] Nevertheless, we do not exclude electric field effects promoted by the close-packed NC arrangement. A recent structural study on Cu_2S supercrystals pointed out the presence of a dipole moment across the [001] direction in single Cu_2S NCs.[16] This intrinsic dipole could promote the formation of supercrystals and in turn may influence the optical transitions. In such a case local fields may lead to the shift of the direct optical transition by the quantum confined Stark-effect, though those might be too weak for explaining the observed changes.[24,25] Moreover, being our NCs not in the quantum confinement regime, electric field effects should be more appropriately described by the Franz−Keldysh effect of bulk semiconductors. Interestingly, in the spectra of Figure 3, we also observe a blue-shift of the near-infrared plasmon band, ascribed to positive free carrier absorption as mentioned above, upon supercrystal deassembly. Plasmon coupling is a known phenomenon in metallic nanoparticles that occurs when the interparticle separation distance is small,[26] giving rise to a red-shift of the plasmon band with respect to the noninteracting particles. The above observation not only highlights further on the relevance of nanocrystal close-packing in our supercrystals, but also points to a possible dipole coupling between the nanoparticle photoexcitations. Further work considering additional spectroscopic techniques such as electro-absorption and photoinduced absorption spectroscopy is needed to identify the role of electric fields on the improved absorption of $Cu_{1.97}S$ supercrystals in the visible range. In this context, we also do not exclude the influence of compositional changes within the NCs upon modifications in their environment. This may ultimately affect their absorption properties.

In conclusion, we have shown that the light absorption properties of $Cu_{1.97}S$ NCs change upon arrangement into supercrystals. Our results indicate that the overall change in the absorption profile toward the red part of the visible spectrum is observed upon NC close-packing. This work highlights the possibility to tune the light absorption properties of $Cu_{1.97}S$ NCs in the visible, which may be relevant for the efficiency of solar cells or photoelectrochemical devices based on this material. Implementation in such devices requires the possibility to obtain supercrystals over large areas over different substrates. This has been recently demonstrated for magnetic NCs and is likely to be applicable to copper-sulfide-based nanoparticles or small supercrystals.[27]

■ ASSOCIATED CONTENT

Supporting Information. HRTEM and selected area electron diffraction (SAED) pattern of the $Cu_{1.97}S$ supercrystals (Figure S1). XRD pattern of the supercrystals before and after the deassembly process (Figure S2). This material is available free of charge via the Internet at http://pubs.acs.org.

■ AUTHOR INFORMATION

Corresponding Author
*E-mail: enrico.dacomo@physik.uni-muenchen.de.

■ ACKNOWLEDGMENT

We thank T. Bein and M. Döblinger, for helpful discussions and support on the experimental equipment. The Nanosystems Initiative Munich (NIM) and the LMUexcellent program of the DFG are kindly acknowledged. E.d.C. and I.K. acknowledge the support from the BMBF project OPV-Stabilität. A.A.L. is grateful to the EU commission for funding via the Marie-Curie research training network ICARUS.

■ REFERENCES

(1) Wadia, C.; Alivisatos, A. P.; Kammen, D. M. *Environ. Sci. Technol.* **2009**, *43*, 2072.
(2) Riha, S. C.; Parkinson, B. A.; Prieto, A. L. *J. Am. Chem. Soc.* **2009**, *131*, 12054.
(3) Steinhagen, C.; Panthani, M. G.; Akhavan, V.; Goodfellow, B.; Koo, B.; Korgel, B. A. *J. Am. Chem. Soc.* **2009**, *131*, 12554.
(4) Schafferhans, J.; Baumann, A.; Deibel, C.; Dyakonov, V. *Appl. Phys. Lett.* **2008**, 93.
(5) Gross, D.; Mora-Sero, I.; Dittrich, T.; Belaidi, A.; Mauser, C.; Houtepen, A. J.; Da Como, E.; Rogach, A. L.; Feldmann, J. *J. Am. Chem. Soc.* **2010**, *132*, 5981.
(6) Kamat, P. V. *J. Phys. Chem. C* **2008**, *112*, 18737.
(7) Johnston, K. W.; Pattantyus-Abraham, A. G.; Clifford, J. P.; Myrskog, S. H.; MacNeil, D. D.; Levina, L.; Sargent, E. H. *Appl. Phys. Lett.* **2008**, 92.
(8) Wu, Y.; Wadia, C.; Ma, W. L.; Sadtler, B.; Alivisatos, A. P. *Nano Lett.* **2008**, *8*, 2551.
(9) Choi, S. H.; An, K.; Kim, E. G.; Yu, J. H.; Kim, J. H.; Hyeon, T. *Adv. Funct. Mater.* **2009**, *19*, 1645.
(10) Talapin, D. V.; Lee, J. S.; Kovalenko, M. V.; Shevchenko, E. V. *Chem. Rev.* **2010**, *110*, 389.
(11) Murray, C. B.; Kagan, C. R.; Bawendi, M. G. *Science* **1995**, *270*, 1335.
(12) Murray, C. B.; Kagan, C. R.; Bawendi, M. G. *Annu. Rev. Mater. Sci.* **2000**, *30*, 545.
(13) Chanyawadee, S.; Lagoudakis, P. G.; Harley, R. T.; Charlton, M. D. B.; Talapin, D. V.; Huang, H. W.; Lin, C. H. *Adv. Mater.* **2010**, *22*, 602.

(14) Baranov, D.; Fiore, A.; van Huis, M.; Giannini, C.; Falqui, A.; Lafont, U.; Zandbergen, H.; Zanella, M.; Cingolani, R.; Manna, L. *Nano Lett.* **2010**, *10*, 743.
(15) Zanella, M.; Bertoni, G.; Franchini, I. R.; Brescia, R.; Baranov, D.; Manna, L. *Chem. Commun.* **2011**, *47*, 203.
(16) Zhuang, Z. B.; Peng, Q.; Zhang, B.; Li, Y. D. *J. Am. Chem. Soc.* **2008**, *130*, 10482.
(17) Zhao, Y. X.; Pan, H. C.; Lou, Y. B.; Qiu, X. F.; Zhu, J. J.; Burda, C. *J. Am. Chem. Soc.* **2009**, *131*, 4253.
(18) Mulder, B. J. *Phys. Staus Solidi A* **1973**, *15*, 409.
(19) Günzler, H.; Gremlich, H.-U. *IR Spectroscopy*; Wiley-VCH Verlag: Weinheim, Germany, 2002.
(20) Lukashev, P.; Lambrecht, W. R. L.; Kotani, T.; van Schilfgaarde, M. *Phys. Rev. B* **2007**, *76*, 195202.
(21) Vossmeyer, T.; Katsikas, L.; Giersig, M.; Popovic, I. G.; Diesner, K.; Chemseddine, A.; Eychmuller, A.; Weller, H. *J. Phys. Chem.* **1994**, *98*, 7665.
(22) Gnutzman., U; Clauseck., K *Applied Physics* **1974**, *3*, 9.
(23) Zachai, R.; Eberl, K.; Abstreiter, G.; Kasper, E.; Kibbel, H. *Phys. Rev. Lett.* **1990**, *64*, 1055.
(24) Empedocles, S. A.; Bawendi, M. G. *Science* **1997**, *278*, 2114.
(25) Miller, D. A. B.; Chemla, D. S.; Damen, T. C.; Gossard, A. C.; Wiegmann, W.; Wood, T. H.; Burrus, C. A. *Phys. Rev. Lett.* **1984**, *53*, 2173.
(26) Jain, P. K.; Huang, W. Y.; El-Sayed, M. A. *Nano Lett.* **2007**, *7*, 2080.
(27) Bodnarchuk, M. I.; Kovalenko, M. V.; Pichler, S.; Fritz-Popovski, G.; Hesser, G.; Heiss, W. *ACS Nano* **2010**, *4*, 423.